Multiple developmental programs are altered by loss of *Zic1* and *Zic4* to cause Dandy-Walker malformation cerebellar pathogenesis

Marissa C. Blank[1], Inessa Grinberg[2], Emmanuel Aryee[3], Christine Laliberte[4], Victor V. Chizhikov[5], R. Mark Henkelman[4] and Kathleen J. Millen[5,6,*]

SUMMARY

Heterozygous deletions encompassing the *ZIC1;ZIC4* locus have been identified in a subset of individuals with the common cerebellar birth defect Dandy-Walker malformation (DWM). Deletion of *Zic1* and *Zic4* in mice produces both cerebellar size and foliation defects similar to human DWM, confirming a requirement for these genes in cerebellar development and providing a model to delineate the developmental basis of this clinically important congenital malformation. Here, we show that reduced cerebellar size in *Zic1* and *Zic4* mutants results from decreased postnatal granule cell progenitor proliferation. Through genetic and molecular analyses, we show that *Zic1* and *Zic4* have Shh-dependent function promoting proliferation of granule cell progenitors. Expression of the Shh-downstream genes *Ptch1*, *Gli1* and *Mycn* was downregulated in *Zic1/4* mutants, although *Shh* production and Purkinje cell gene expression were normal. Reduction of Shh dose on the *Zic1+/–;Zic4+/–* background also resulted in cerebellar size reductions and gene expression changes comparable with those observed in *Zic1–/–;Zic4–/–* mice. *Zic1* and *Zic4* are additionally required to pattern anterior vermis foliation. *Zic* mutant folial patterning abnormalities correlated with disrupted cerebellar anlage gene expression and Purkinje cell topography during late embryonic stages; however, this phenotype was Shh independent. In *Zic1+/–;Zic4+/–;Shh+/–*, we observed normal cerebellar anlage patterning and foliation. Furthermore, cerebellar patterning was normal in both *Gli2-cko* and *Smo-cko* mutant mice, where all Shh function was removed from the developing cerebellum. Thus, our data demonstrate that *Zic1* and *Zic4* have both Shh-dependent and -independent roles during cerebellar development and that multiple developmental disruptions underlie *Zic1/4*-related DWM.

KEY WORDS: Dandy-Walker malformation, Cerbellum, Foliation, Proliferation

INTRODUCTION

Dandy-Walker malformation (DWM) is the most common congenital cerebellar malformation in humans, estimated to occur in 1/5000 live births (Parisi and Dobyns, 2003). DWM is characterized by reduced cerebellar vermis size, rotation of the vermis away from the brain stem and a large posterior fossa (Barkovich et al., 2009), and is also often associated with mild to severe ataxia and developmental delay. Low familial recurrence rates suggest that DWM is polygenic, with strong support for at least four genetic loci (Aldinger et al., 2009; Grinberg et al., 2004; Jalali et al., 2008; McCormack et al., 2002). Characterization of two of these loci has identified three DWM causative genes: *FOXC1* on human chromosome 6p25 (Aldinger et al., 2009) and the linked *ZIC1* and *ZIC4* genes on human chromosome 3q24. Mice that are heterozygous null for both *Zic1* and *Zic4* model human DWM, although the developmental basis of this phenotype remains unknown (Grinberg et al., 2004).

Zic1 and *Zic4* belong to the family of five Zic genes, each encoding a highly related zinc-finger (ZF) transcription factor. The Zic genes are broadly expressed in overlapping patterns during embryogenesis and each member has been documented to have numerous roles, including cerebellar development (Aruga et al., 2002a; Aruga et al., 1998; Aruga et al., 2004; Grinberg et al., 2004). Although few transcriptional targets of *Zic* genes have been identified (Merzdorf, 2007), the Zic family ZF domains are very similar to Gli family ZF domains. As Gli proteins are crucial downstream mediators of Shh signaling (Ruiz i Altaba et al., 2002; Vaillant and Monard, 2009) and as they physically interact with Zics proteins in vitro, this has lead to the hypothesis that Zic proteins compete or interact with Gli proteins to regulate Shh signaling (Ishiguro et al., 2004; Koyabu et al., 2001; Mizugishi et al., 2001). The roles of *Zic1* and *Zic4* in Shh signaling have never been directly assessed in vivo.

Shh signaling is crucial for normal cerebellar development. Shh secreted from Purkinje cells (PCs) within the perinatal cerebellar anlage drives expansion of the overlying granule cell progenitor (GCP) population resulting in rapid cerebellar growth during the first postnatal weeks in mice (Corrales et al., 2006; Lewis et al., 2004; Vaillant and Monard, 2009). The *Zic1+/–;Zic4+/–* mutant cerebellar phenotype (Grinberg et al., 2004) is superficially similar to *Smo* and *Gli2* conditional knockouts, which display small cerebella and simplified cerebellar foliation (Corrales et al., 2006). Given the hypothesized roles of Zic genes in regulating Gli function, we initiated an extensive developmental analysis to determine whether altered Shh signaling was central to *Zic1/4*-dependent DWM pathogenesis.

[1]Departments of Molecular Genetics and Cell Biology, The University of Chicago, Chicago, IL 60637, USA. [2]Human Genetics, The University of Chicago, Chicago, IL 60637, USA. [3]The College, The University of Chicago, Chicago, IL 60637, USA. [4]The Mouse Imaging Centre (MICE), SickKids, 25 Orde Street, Toronto, ON M5T 3H7, Canada. [5]Seattle Children's Hospital Research Institute, 1900 Ninth Avenue, Seattle, WA 98101 USA. [6]The University of Washington, Department of Pediatrics,1900 Ninth Avenue, Seattle, WA 98101 USA.

*Author for correspondence (kathleen.millen@seattlechildrens.org)

In this study, we demonstrate that *Zic1* and *Zic4* have Shh-dependent roles in postnatal cerebellar GCP proliferation. We also show that Shh pathway mutant cerebellar phenotypes are similar to, but distinct from, *Zic1* and *Zic4* mutant phenotypes, indicating additional roles for *Zic1* and *Zic4* outside of the Shh pathway in anterior vermis cardinal fissure formation and the patterning of PC topography in the embryonic cerebellar anlage.

MATERIALS AND METHODS

Mice

Animals were treated in accordance with an IACUC approved protocol. $Zic1^{+/-}$ (Aruga et al., 1998), $Zic4^{+/-}$, $Zic1^{+/-};Zic4^{+/-}$ (Grinberg et al., 2004) and $Shh^{+/-}$ mice (Chiang et al., 1996) were maintained on a 129S1/SvImJ background and $Gli2^{+/flox};En1-cre$ and $Gli2^{+/zfd}$ mice were maintained on a CD1 background (Corrales et al., 2006) with genotyping performed as previously described in these references.

BrdU incorporation, immunohistochemistry and histology

Pregnant dams or P0 and P1 pups were injected intraperitoneally with 1.0 or 0.1 ml BrdU labeling reagent (Invitrogen) and sacrificed after 30 minutes. Brains were fixed and cryopreserved as previously described (Chizhikov and Millen, 2004). Sagittal cryosections (12 μm) were collected across the cerebellar vermis. Antigen retrieval for immunohistochemistry was performed with target retrieval solution (DAKO) according to the manufacturer instructions. Following this, antibody staining was performed as previously described (Chizhikov and Millen, 2004) and antibodies were as follows: Zic1 (rabbit polyclonal, Rockland Immunochemicals), GABA$_A$ receptor α6 (rabbit polyclonal, Chemicon), calbindin (rabbit polyclonal, Swant), and Tag1 and BrdU (both mouse monoclonal, Developmental Studies Hybridoma Bank). Species-appropriate Alexa 568-conjugated secondary antibodies (Invitrogen) and DAPI (Sigma) counterstain were also used.

For histology, brains were fixed in 4% PFA for at least 24 hours, sunk in either 30% sucrose/PBS or 30% sucrose/formalin and embedded in either OCT or gelatin. Cresyl Violet staining of 20 μm sections was performed according to standard protocols.

Cell counts and statistics

Anti-BrdU+ DAPI stained sections were photographed for area measurements and cell counts. Morphological landmarks from each section were used to distinguish vermis from hemispheres and only cerebellar vermis sections were analyzed. Three regions of the external granule layer (EGL) corresponding to the preculminate, primary and secondary fissures were chosen for cell counts. Cell counts and area measurements were performed in Image J (http://rsbweb.nih.gov/ij/). For each age and genotype (*n*=4 animals, *n*>6 sections/animal, *n*>1850 counted cells/animal), statistical significance was determined using a paired *t*-test.

Whole-mount immunohistochemistry and in situ hybridization

Whole-mount immunohistochemistry was performed as previously described (Sillitoe and Hawkes, 2002). P3 and E17.5 cerebella were stained using anti-Plcβ4 (rabbit polyclonal, Santa Cruz) and a biotin-SP-conjugated secondary antibody (Jackson ImmunoResearch) with a Vectastain ABC peroxidase kit (Vector Laboratories).

In situ hybridization was performed as previously described (Chizhikov and Millen, 2004) using digoxigenin-labeled riboprobes to mouse *Zic1*, *Zic4*, *Wnt7b* and *Epha4* (Grinberg et al., 2004; Liebl et al., 2003; Nagai et al., 1997; Parr et al., 1993).

MRI and volumetric analysis

As previously described (Spring et al., 2007), P33 to P40 mice were anesthetized with Euthasol (Delmarva Laboratories) and transcardially perfused with PBS and PFA containing 2 mM Prohance (Bracco Diagnostics). Imaging and analysis were also performed as described in the above reference and analysis of variance (ANOVA) was used to identify significant differences in brain structure size.

RNA extraction and quantitative RT-PCR

RNA was extracted from whole, flash frozen cerebella using the RNeasy extraction kit with Qiashredder and gDNA eliminator columns (Qiagen) according to manufacturer protocols. cDNA was reverse transcribed with a SuperscriptII kit (Invitrogen) and quantitative (q) RT-PCR was performed with Sybr Green master mix (BioRad) in an iQ5 iCycler (BioRad). Primers were designed to amplify 100-200 bp unique regions of genes analyzed, spanning splice sites when possible. Primer sequences were obtained either from primer depot (http://mouseprimerdepot.nci.nih.gov/) or were designed using primer3 software (http://frodo.wi.mit.edu/primer3/input.htm) (sequences available upon request). *Gapdh* was used as a reference gene to calculate $2^{(-\Delta\Delta ct)}$ and experiments were performed with three biological replicates on at least four samples per genotype and age examined.

RESULTS

Zic gene dose determines severity of cerebellar abnormalities and ataxia

We previously reported the cerebellar phenotypes of $Zic1^{+/-};Zic4^{+/-}$ mice, which model human chromosome 3q24 deletion DWM (Grinberg et al., 2004). Here, we report the mouse phenotypes associated with a complete allelic series of all *Zic1*- and *Zic4*-null genotypes.

$Zic1^{-/-}$, $Zic4^{-/-}$ and $Zic1^{-/-};Zic4^{-/-}$ mutant mice, generated by heterozygote mating, were all born at expected Mendelian frequencies. $Zic4^{-/-}$ pups were slightly smaller than wild-type littermates but were otherwise indistinguishable by behavior or viability. $Zic1^{-/-}$ mutants (Aruga et al., 1998), and $Zic1^{-/-};Zic4^{-/-}$ mutants were markedly smaller than wild-type and heterozygous littermates from postnatal day 5 (P5) onwards (data not shown). At two postnatal weeks, both groups of mutants had failed to develop the righting reflex, a characteristic sign of cerebellar ataxia. There was no discernible difference in either relative size or righting reflex between $Zic1^{-/-}$ and $Zic1^{-/-};Zic4^{-/-}$ pups, and further quantitative behavioral assessment was not possible due to the severity of the phenotype. Neither $Zic1^{-/-}$ nor $Zic1^{-/-};Zic4^{-/-}$ mice survived past weaning age.

Analysis of whole mutant cerebella and sagittal vermis sections revealed that $Zic4^{-/-}$ cerebellar size was slightly reduced compared with wild type (Fig. 1A,B), whereas foliation was grossly normal (Fig. 1E,F). $Zic1^{-/-}$ cerebella were small compared with wild type, most notably along the anterior-posterior (AP) axis (Fig. 1C), and sections through the vermis showed the loss of one folium anterior to the primary fissure (Fig. 1G). $Zic1^{-/-};Zic4^{-/-}$ cerebella were smaller than wild type, $Zic4^{-/-}$ and $Zic1^{-/-}$ cerebella with respect to AP and medial-lateral (ML) axes (Fig. 1D), and also exhibited loss of one anterior folium (Fig. 1H).

Analysis of a complete allelic series of *Zic1* and *Zic4* mutants revealed that phenotypic severity was dependent on *Zic1* and *Zic4* dose as mutant viability and cerebellar phenotype worsened progressively with loss of Zic alleles (see Fig. S1 in the supplementary material). $Zic4^{+/-}$ and $Zic1^{+/-}$ mice (see Fig. S1B,C in the supplementary material) had no gross behavioral or cerebellar morphological defects, and had normal viability. As we previously described, 15% of $Zic1^{+/-};Zic4^{+/-}$ mice (see Fig. S1H in the supplementary material) had a severe cerebellar phenotype similar to $Zic1^{-/-};Zic4^{-/-}$ mutants (see Fig. S1K in the supplementary material) (Grinberg et al., 2004). In this study, 40% of $Zic1^{+/-};Zic4^{-/-}$ mice also had the severe cerebellar phenotype with hypoplasia and loss of an anterior folium (see Fig. S1G in the supplementary material), while 60% appeared normal (see Fig. S1F in the supplementary material). Additional factors that contribute to phenotypic variability in $Zic1^{+/-};Zic4^{\pm/-}$ cerebella remain to be identified; however, these data indicate that *Zic1* and *Zic4* interact
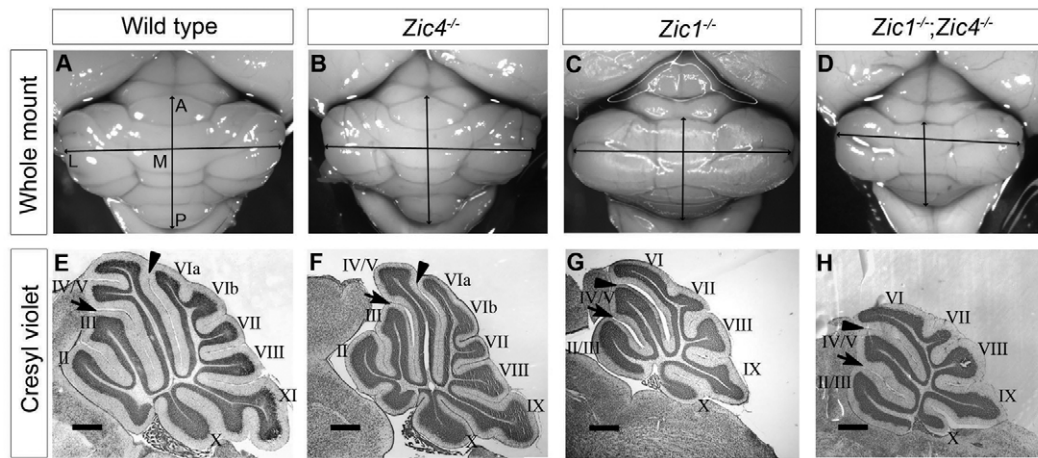
**Fig. 1. *Zic1* and *Zic4* mutants have cerebellar size and foliation defects.** (**A-D**) Dorsal views of whole P20 cerebella show that *Zic4*$^{-/-}$ (B) cerebella were slightly smaller than wild type (A). *Zic1*$^{-/-}$ (C) and *Zic1*$^{-/-}$;*Zic4*$^{-/-}$ (D) cerebella were much smaller than wild type along the anterior-posterior (AP) axis and *Zic1*$^{-/-}$;*Zic4*$^{-/-}$ cerebella were also smaller along the medial-lateral (ML) axis. (**E-H**) Cresyl Violet-stained sagittal sections through the cerebellar vermis. Black arrowheads and arrows indicate the primary and preculminate fissures, respectively, and folia are labeled with roman numerals (II-X). Wild-type (E) and *Zic4*$^{-/-}$ (F) cerebella had three folia anterior to the primary fissure, whereas *Zic1*$^{-/-}$ (G) and *Zic1*$^{-/-}$;*Zic4*$^{-/-}$ (H) cerebella were dramatically hypoplastic, were missing one anterior folium and lacked a fissure between folia VIa and VIb. Scale bars: 500 µm in E-H.

genetically to regulate cerebellar development in a dose-sensitive manner. To avoid the complexity of variable phenotypes, all subsequent analyses of *Zic1* and *Zic4* function were performed in homozygous mutants.

## *Zic1* and *Zic4* are expressed throughout cerebellar development

To determine how *Zic1* and *Zic4* regulate cerebellar development, we conducted a detailed analysis of their developmental expression profiles. Confirming and extending previously published analyses (Aruga et al., 1998), we found scattered Zic1 expression in cells throughout both the developing white matter and internal granule cell layer (IGL) and strong expression in the external granule layer (EGL) (Fig. 2A) at P1 in wild type. No Zic1 expression was

detected anywhere in the brain using this antibody in *Zic1*$^{-/-}$ animals, demonstrating antibody specificity (data not shown). As no Zic4-specific antibody was available, we used in situ hybridization to characterize expression of this gene. We detected strong *Zic4* expression in the EGL as well as the anterior IGL of the cerebellar cortex, with additional scattered staining throughout the remaining cerebellum at P1 (Fig. 2B). At embryonic day 17.5 (E17.5), *Zic1* and *Zic4* were broadly expressed throughout the entire cerebellar anlage (Fig. 2C,D). At E12.5, *Zic1* and *Zic4* were both expressed along the entire ML extent of the cerebellar anlage (Fig. 2E-H); however, although both Zic1 and Zic4 were expressed in the cerebellar rhombic lip and adjacent mesenchyme, Zic1 expression alone extended through the cerebellar ventricular zone (VZ), the source of several cell types, including PCs (Fig. 2I,J).
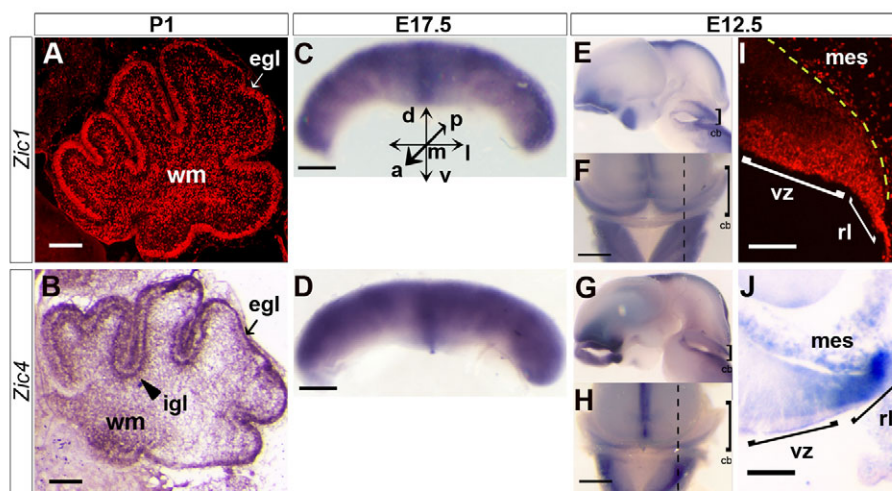
Fig. 2. *Zic1* and *Zic4* have dynamic expression patterns throughout cerebellar development. (**A,B**) P1 cerebellar sagittal sections: *Zic1* and *Zic4* were expressed in the cerebellar external granule layer (egl, arrow) and white matter (wm), and *Zic4* was also expressed in the internal granule cell layer (igl, arrowhead). (**C,D**) Anterior view of whole cerebellum at E17.5; *Zic1* and *Zic4* were broadly expressed in the embryonic cerebellum. d, dorsal; v, ventral; a, anterior; p, posterior; m, medial; l, lateral. (**E-H**) Whole-mount lateral (E,G) and dorsal (F,H) views of the E12.5 cerebellar region (cb, brackets) with dotted lines (F,H) indicating the level of E12.5 sagittal sections in I,J. (**I,J**) *Zic1* and *Zic4* were both expressed in the cerebellar rhombic lip (rl) and mesenchyme (mes), with Zic1 also expressed in the ventricular zone (vz). Scale bars: 500 µm in A-H; 100 µm in I,J.
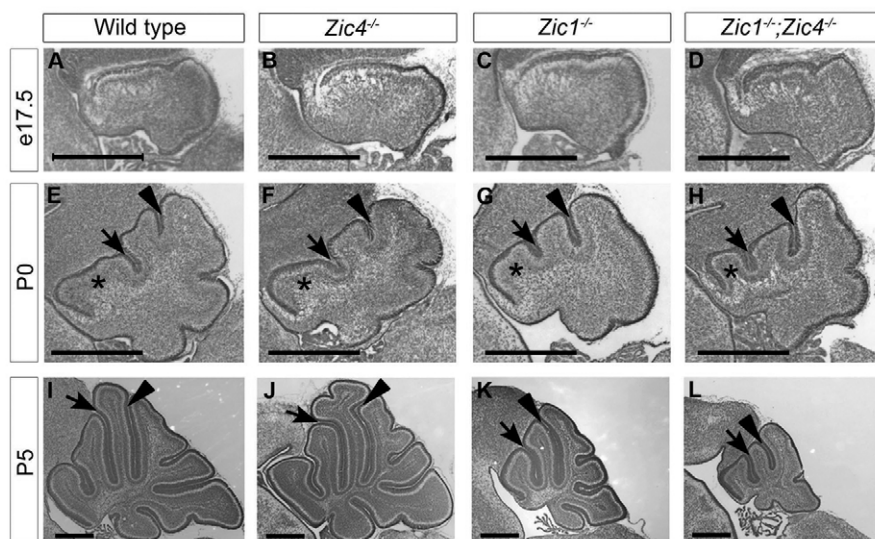
Fig. 3. *Zic1* and *Zic4* cerebellar size and foliation defects arise postnatally.
(**A-D**) Cresyl Violet stained sections showed no gross cerebellar morphological defects at E17.5 in single or double homozygous mutants (B-D) compared with wild type (A). (**E-L**) At P0, each genotype had the correct number of cardinal fissures, but while the *Zic4*$^{-/-}$ mutant (F) resembled wild type (E), in *Zic1*$^{-/-}$ (F) and *Zic1*$^{-/-}$;*Zic4*$^{-/-}$ (G) mutants the preculminate fissure was shifted anteriorly and the anterobasal lobe (asterisk) was smaller than wild type. By P5, both the wild-type (I) and *Zic4*$^{-/-}$ mutant (J) cerebella had grown considerably, whereas *Zic1*$^{-/-}$ (F) and *Zic1*$^{-/-}$;*Zic4*$^{-/-}$ (G) cerebella remained small. Black arrowheads and arrows indicate the primary and preculminate fissures, respectively. Scale bars: 500 µm.

Cerebellar size and foliation defects appear during early postnatal development in *Zic1*/*Zic4* mutant mice

We next conducted a developmental analysis of *Zic1* and *Zic4* homozygous mutants. In all mutants, cerebellar anatomy was grossly normal at E17.5 (Fig. 3A-D) with no discernible changes in size, shape, tissue organization or cell morphology. However, at P0, when the cardinal fissures of the cerebellum were apparent (Sillitoe and Joyner, 2007), differences between wild type and the *Zic* mutants became evident. Notably, in both *Zic1*$^{-/-}$ and *Zic1*$^{-/-}$;*Zic4*$^{-/-}$ mutant cerebella (Fig. 3G,H), the preculminate fissure (arrow) was shifted anteriorly compared with wild type or *Zic4*$^{-/-}$ mutants (Fig. 3E,F). As a result, the anterobasal lobe (asterisk in Fig. 3E-H) was reduced in size and it was from this region that one folium was missing in adult *Zic1*$^{-/-}$ and *Zic1*$^{-/-}$;*Zic4*$^{-/-}$ mutants (Fig. 1G,H). By P5, wild-type and *Zic4*$^{-/-}$ cerebella had three anterior folia and had grown considerably, whereas *Zic1*$^{-/-}$ and *Zic1*$^{-/-}$;*Zic4*$^{-/-}$ cerebella had only two anterior folia and remained small (Fig. 3I-L).

To quantify cerebellar growth during early postnatal development, we measured mid-sagittal cerebellar vermis area at P0, P1 and P5 for each mutant genotype (Fig. 4A; data not shown). Area measurements for each mutant were not statistically different from wild type at P0. However, at P1, *Zic1*$^{-/-}$ and *Zic1*$^{-/-}$;*Zic4*$^{-/-}$ cerebella were nearly 40% smaller than wild type, and size differences persisted through P5. A comparison of P0 and P1 values within genotypes showed that, whereas wild-type cerebellar area increased by 38%, virtually no growth was observed in the sagittal plane in *Zic1*$^{-/-}$ and *Zic1*$^{-/-}$;*Zic4*$^{-/-}$ mutants.
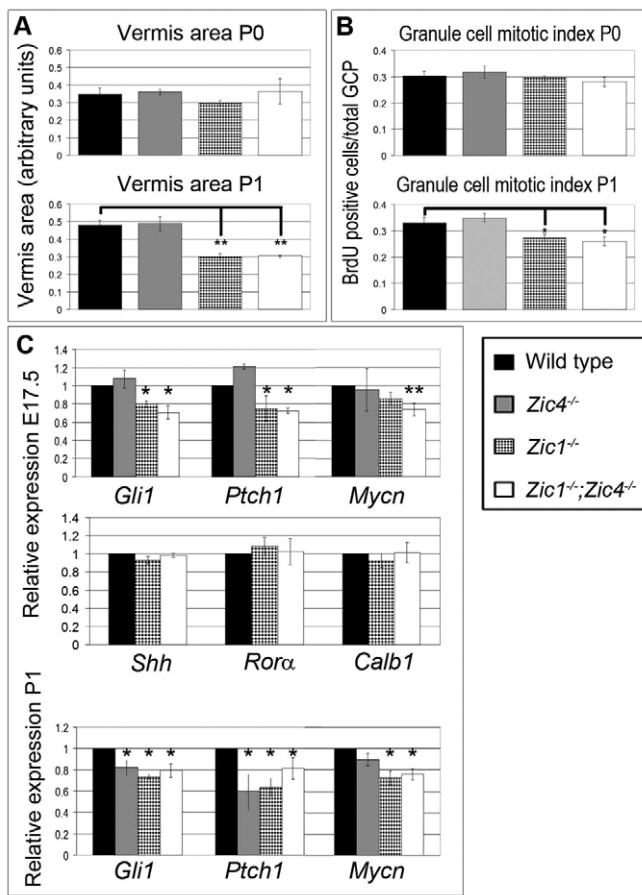
Reduced granule cell proliferation correlates with decreased Shh target gene expression to contribute to reduced cerebellar size

Early postnatal cerebellar growth is predominantly due to rapid proliferation of the EGL (Porgoriler et al., 2006; Vaillant and Monard, 2009) and as *Zic1* and *Zic4* are highly expressed in EGL cells (Fig. 2A,B), we assessed EGL proliferation by BrdU incorporation analysis. Although unchanged from wild type at P0, the mitotic indices of the EGL in *Zic1*$^{-/-}$ and *Zic1*$^{-/-}$;*Zic4*$^{-/-}$ cerebella were significantly reduced by 18-22% (*P*<0.05) at P1 (Fig. 4B). To rule out the possibility that premature granule cell (GC) differentiation contributed to reduced cerebellar size, we also

performed antibody staining of P0 and P1 sections with antibodies to Tag-1 and Gaba-α6. Neither marker of GC differentiation was expressed at the stages examined (data not shown), supporting our hypothesis that the main cause of mutant cerebellar size defects was reduced EGL proliferation.

As postnatal EGL expansion is primarily driven by Shh signaling from the underlying PC layer (Vaillant and Monard, 2009), we next assessed whether the Shh pathway was disrupted in our mutants. Shh target gene expression was measured by qRT-PCR (Fig. 4C). At E17.5, *Gli1* and *Ptch1* expression were significantly reduced in *Zic1*$^{-/-}$ and *Zic1*$^{-/-}$;*Zic4*$^{-/-}$ cerebella (*P*<0.05). *Mycn* was also reduced in *Zic1*$^{-/-}$;*Zic4*$^{-/-}$ cerebella (*P*<0.05). At P1, *Gli1* and *Ptch1* expression were significantly reduced in *Zic1*$^{-/-}$, *Zic4*$^{-/-}$ and *Zic1*$^{-/-}$;*Zic4*$^{-/-}$ cerebella (*P*<0.05), whereas *Mycn* was reduced in *Zic1*$^{-/-}$ and *Zic1*$^{-/-}$;*Zic4*$^{-/-}$ (*P*<0.05), but not in *Zic4*$^{-/-}$, cerebella. Reduced expression of Shh targets suggested that the Shh pathway was compromised in *Zic1*$^{-/-}$, *Zic1*$^{-/-}$;*Zic4*$^{-/-}$, and to a lesser extent *Zic4*$^{-/-}$ cerebella. Although EGL cells in *Zic1*$^{-/-}$ and *Zic1*$^{-/-}$;*Zic4*$^{-/-}$ cerebella had a reduced response to Shh signaling, analysis of *Shh* itself as well as of *Rora* and *Calb1*, all of which are expressed in PCs, showed that mRNA levels were unaffected in *Zic1*$^{-/-}$ and *Zic1*$^{-/-}$;*Zic4*$^{-/-}$ cerebella, further demonstrating that PCs were unaffected in these mutants (Fig. 4C).

To determine whether disruption of other pathways contributed to reduced perinatal EGL proliferation, we performed qRT-PCR at E17.5 and P1 for *Bmp2*, *Bmp4*, *Fgf2*, *Fgf8*, *Wnt1*, *Igf2* and *Igfr1*, all of which have been demonstrated to regulate EGL proliferation (Behesti and Marino, 2009). *Bmp2* and *Bmp4*, which antagonize the Shh pathway and promote GC differentiation, were not significantly upregulated at E17.5, whereas *Bmp2* expression was slightly elevated in *Zic1*$^{-/-}$;*Zic4*$^{-/-}$ at P1, expression was not significantly increased in *Zic1*$^{-/-}$ mutants and *Bmp4* expression at P1 was also normal (data not shown), indicating that if Bmps play a role in *Zic* mutant cerebellar abnormalities, it is probably a minor one. Of the remaining genes examined, only *Wnt1* was significantly downregulated in *Zic1*$^{-/-}$ and *Zic1*$^{-/-}$;*Zic4*$^{-/-}$ mutants at E17.5; however, this was not observed at P1 (data not shown). We also found no evidence of altered expression of GC genes such as *Pax6* and *Ru49* (*Zscan21* – Mouse Genome Informatics) (data not shown). These data indicate that general GC health and identity were not affected in our mutants, suggesting a specific deficit in the Shh pathway.

Fig. 4. Reduced cerebellar size and granule cell proliferation correlate with expression of Shh target genes. (**A**) Cross-sectional area of cerebellar vermis was similar for all genotypes at P0. By P1, $Zic1^{-/-}$ and $Zic1^{-/-};Zic4^{-/-}$ cerebellar vermis areas were significantly smaller than those of wild-type or $Zic4^{-/-}$ animals (**$P<0.01$). (**B**) Mitotic index was calculated by total number of BrdU-positive (GCP)/total GCP. By P1, $Zic1^{-/-}$ and $Zic1^{-/-};Zic4^{-/-}$ had significantly reduced EGL proliferation compared with wild-type or $Zic4^{-/-}$ animals (*$P<0.05$). (**C**) Expression of Shh target genes $Gli1$, $Ptch1$ and $Mycn$ was significantly reduced in $Zic1^{-/-}$ and $Zic1^{-/-};Zic4^{-/-}$ whole cerebella at E17.5, whereas Shh, $Calb1$ and $Rora$ expression levels remained normal. Expression of $Gli1$ and $Ptch1$ was significantly reduced for all mutants at P1 (*$P<0.05$, **$P<0.01$). Data are mean±s.e.m.

Zic1 and Zic4 regulate cerebellar size via a Shh-dependent pathway

Zic proteins have long been hypothesized to regulate Gli-mediated Shh signaling (Koyabu et al., 2001). Our proliferation and expression data confirmed downregulation of Shh pathway components in $Zic1^{-/-}$ and $Zic1^{-/-};Zic4^{-/-}$ mutant cerebella, with the additional possible contribution of reduced $Wnt1$ expression at E17.5. To directly test the extent to which $Zic1$ and $Zic4$ interact with the Shh pathway, we crossed $Shh^{+/-}$ mice to $Zic1^{+/-};Zic4^{+/-}$ mutants to produce triple heterozygotes. We hypothesized that if the Zics function within the Shh pathway, reduced Shh expression on the $Zic1^{+/-};Zic4^{+/-}$ background would be sufficient to cause a severe cerebellar phenotype similar to that observed in $Zic1^{-/-};Zic4^{-/-}$ mice. $Zic1^{+/-};Zic4^{+/-};Shh^{+/-}$ pups were born at expected Mendelian frequencies, and were comparable in size and behavior with wild-type littermates. Notably, histological analysis

of $Zic1^{+/-};Zic4^{+/-};Shh^{+/-}$ animals revealed the correct number of normally patterned cerebellar folia (Fig. 5D); however, the area of cerebellar vermis sections was decreased, similar to the size reduction in $Zic1^{-/-};Zic4^{-/-}$ animals.

MRI followed by 3D reconstruction was employed to quantify cerebellar size differences. The results showed significant differences in cerebellar size ($f>17$, $P<0.0001$) between wild type and the three groups of heterozygotes: $Zic1^{+/-};Zic4^{+/-}$ and $Shh^{+/-}$ cerebella were smaller than wild type. Notably, $Zic1^{+/-};Zic4^{+/-};Shh^{+/-}$ cerebella were significantly smaller than either $Zic1^{+/-};Zic4^{+/-}$ or $Shh^{+/-}$ cerebella ($P<0.0024$) (Fig. 5H). The cerebellum was disproportionately affected relative to total brain volume and structures such as the frontal lobes were not significantly different across genotypes ($f=1.53$, $P=0.22$). Thus, the $Zic1^{+/-};Zic4^{+/-}$ cerebellar size phenotype was exacerbated by reduced Shh expression. To further bolster these findings, we performed qRT-PCR on $Zic1^{+/-};Zic4^{+/-}$, $Shh^{+/-}$ and $Zic1^{+/-};Zic4^{+/-};Shh^{+/-}$ cerebella and found that, whereas $Gli1$ and $Mycn$ were normally expressed in $Zic1^{+/-};Zic4^{+/-}$ and $Shh^{+/-}$ cerebella at E17.5, expression of both genes was reduced in triple heterozygotes. $Ptch1$ expression was reduced in all three genotypes, but was significantly lower in the triple heterozygote (Fig. 5I, $P<0.05$). Our volumetric and expression data supported the conclusion that the cerebellar size reduction seen in $Zic1^{-/-};Zic4^{-/-}$ mutants was the result of a genetic interaction between Zic genes and the Shh pathway.

We observed normal foliation in triple heterozygous mutants, despite decreased size (Fig. 5D); however, these data were insufficient to allow us to state conclusively that the $Zic1/4$ folial patterning phenotype was Shh independent. Homozygous deletion of Shh is lethal by birth, long before completion of cerebellar foliation, making the study of cerebellar foliation in these mutants impossible (Chiang et al., 1996). Conditional deletion of $Gli2$ by $En1^{cre}$ ($Gli2$-cko) has been shown to effectively eliminate Shh activity from the developing cerebellum, while ensuring postnatal viability (Corrales et al., 2006). With these mice, we were able to determine that, despite severe cerebellar hypoplasia, all $Gli2$-cko cerebella ($n=5$) had three folia anterior to the primary fissure (Fig. 5F), similar to wild type (Fig. 5A). In conjunction with our data from $Zic1^{+/-};Zic4^{+/-};Shh^{+/-}$ mice, these observations strongly argue that Zic-mediated patterning of the cardinal folia in the anterior cerebellar anlage is Shh independent.

Zic1 and Zic4 regulate PC compartmentalization independent of the Shh pathway

The loss of one anterior folium in $Zic1^{-/-}$ and $Zic1^{-/-};Zic4^{-/-}$ animals suggested that $Zic1$ and $Zic4$ are important for setting up early patterns in the developing cerebellum that drive normal anterior foliation. Although no known genes mark sites of cardinal fissure formation, a number of genes demonstrate regional patterning at E17.5 (Blanco et al., 2002; Karam et al., 2002; Larouche and Hawkes, 2006; Millen et al., 1995; Sarna et al., 2006) and we hypothesized that patterning of the anterior cerebellar anlage would be abnormal in $Zic1^{-/-}$ and $Zic1^{-/-};Zic4^{-/-}$ mutants at this stage.

In our Zic mutants, some genes, such as $En2$, had normal medial lateral patterning in the embryonic cerebellar anlage (data not shown). However, in situ hybridization with probes to $Wnt7b$ and $Epha4$ showed that stripes of expression present in wild type (Fig. 6A,C) were absent or truncated only in the most anterior regions of $Zic1^{-/-}$ and $Zic1^{-/-};Zic4^{-/-}$ mutant cerebellar vermis (Fig. 6B,D; see Fig. S2B,D,F,H in the supplementary material). Qualitative observations of reduced $Epha4$ expression were bolstered by qRT-
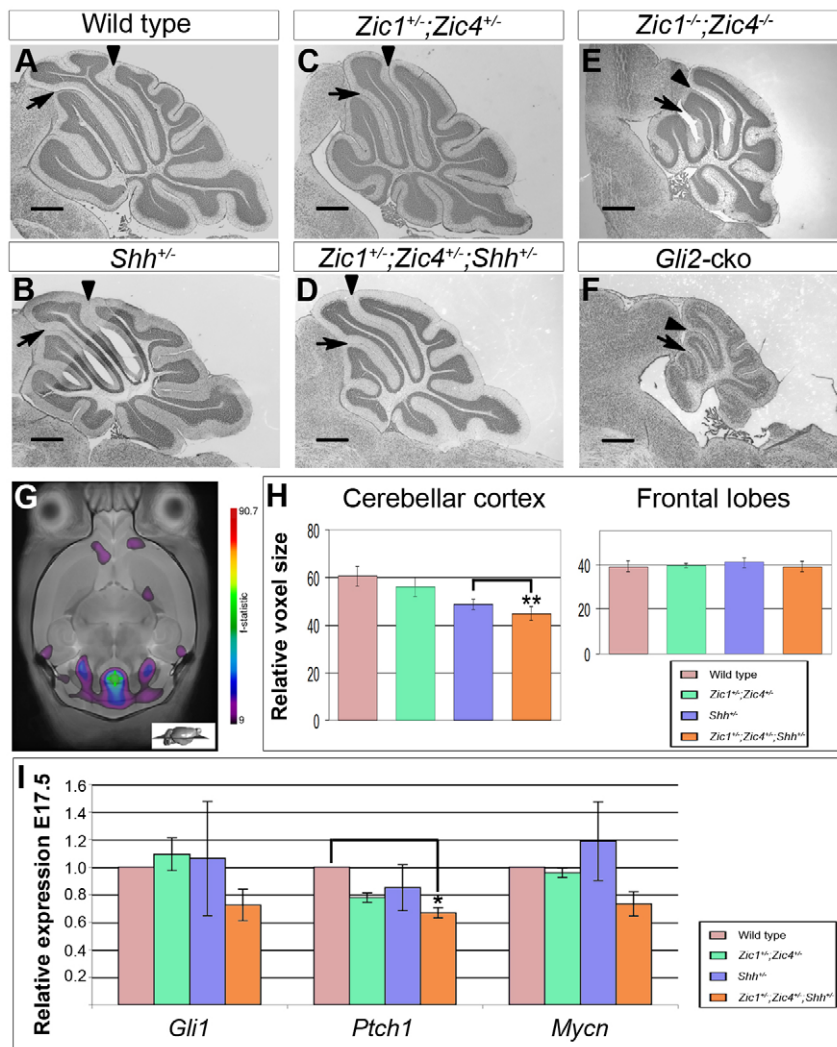
Fig. 5. Zic gene interaction with the Shh pathway controls cerebellar size, but not foliation. (**A-F**) Cresyl Violet-stained sagittal sections through the cerebellar vermis of P20 mice. Black arrowheads and arrows (A-F) indicate the primary and preculminate fissures, respectively. Compared with wild type (A), *Shh*+/– (B) and *Zic1*+/–;*Zic4*+/– (C) cerebellar vermis sections had normal foliation and size. *Zic1*+/–;*Zic4*+/–;*Shh*+/– (D) cerebella also had the correct number of folia, but vermis area was reduced, similar to that of the *Zic1*–/–;*Zic4*–/– mutant (E). The *Gli2*-cko (F) had an extremely hypoplastic cerebellum, but retained three anterior folia. Scale bars: 500 µm. (**G**) Representative horizontal MR image with a heat map indicating regions of size difference that were significant at a false discovery rate of 0.1% in wild type and *Zic1*+/–;*Zic4*+/–;*Shh*+/– brains. (**H**) Quantification of voxels from wild-type, *Zic1*+/–;*Zic4*+/–, *Shh*+/– and *Zic1*+/–;*Zic4*+/–; *Shh*+/– cerebella (*n*=10 per genotype) showed that cerebellar size was significantly reduced in *Zic1*+/–;*Zic4*+/–; *Shh*+/– mice (whole dataset comparison *f*>17, *P*<0.0001; paired *t*-test comparison of *Shh*+/– with *Zic1*+/–;*Zic4*+/–;*Shh*+/– **P*=0.0024). Frontal lobe size did not vary significantly across genotypes (*f*=1.53, *P*=0.22). (**I**) Relative expression of *Gli1*, *Ptch1* and *Mycn* at E17.5 (**P*<0.05). Data are mean±s.e.m.

PCR, which showed a significant decrease in *Epha4* expression in *Zic1*–/– and *Zic1*–/–;*Zic4*–/– mutant cerebella (see Fig. S3 in the supplementary material). Importantly, the patterning of *Epha4* and *Wnt7b* domains was normal in *Zic4*–/–, *Gli2*-cko and *Zic1*+/–;*Zic4*+/–;*Shh*+/– cerebella (see Fig. S2C,G,M-P in the supplementary material), in which adult foliation was normal. *Wnt7b* expression patterns were also normal in E17.5 *Smo*flox;*En1*cre cerebella (data not shown), from which Shh activity is eliminated by E9.0 (Corrales et al., 2006; Kimmel et al., 2000; Li et al., 2002), further indicating that stripe patterning is Shh independent.

Changes in PC gene expression at E17.5 were not transient, but reflected permanent PC patterning defects, as we observed changes in the striped expression of Plcβ4 at P3 in *Zic1*–/– and *Zic1*–/–;*Zic4*–/– mutants; specifically, within the anterior vermis domains of *Zic1*–/– and *Zic1*–/–;*Zic4*–/– cerebella, lateral stripes of expression were disproportionately narrow in lobe II/III and all stripes were disrupted in lobe IV/V (Fig. 6J,K; see Fig. S4A′,C′,D′ in the supplementary material). Despite disrupted expression, PC morphology was normal at all stages in all Zic gene mutants (data not shown).

Our data indicate a correlation between altered patterning of the developing cerebellar anterior vermis and abnormal postnatal foliation in this domain. Although we cannot directly link these phenotypes, our data strongly argue that *Zic1*–/– and *Zic1*–/–;*Zic4*–/– cerebellar patterning phenotypes are Shh independent.

Early patterning and proliferation of the cerebellar anlage is normal in *Zic1* and *Zic4* mutants

We next examined the organization of the cerebellar anlage at E12.5 when *Zic1* is expressed in the cerebellar VZ (Fig. 2I) and PC production is under way (Goldowitz and Hamre, 1998), as the PC 'stripe' and positional identity have been shown to be an intrinsic phenotype that is probably conferred when PCs are generated (Hashimoto and Mikoshiba, 2003; Larouche and Hawkes, 2006). Antibody staining was performed on wild-type and *Zic1*–/–;*Zic4*–/– mutant cerebellar sections at E12.5 using a series of markers that distinguish four cellular populations in dorsal E12.5 rhombomere 1 (Chizhikov et al., 2006). Each population was present in the *Zic1*–/–;*Zic4*–/– mutant cerebellum with expression patterns that were indistinguishable from wild type (Fig. 7B-G). Thus, at this resolution, we found no evidence of abnormal cerebellar patterning at this stage. We also conducted BrdU analysis of the cerebellar VZ to determine whether loss of *Zic1* and *Zic4* altered PC progenitor proliferation similar to its effect on EGL proliferation. No significant differences were observed between wild type and *Zic1*–/–;*Zic4*–/– mutants (Fig. 7H-J). We conclude, therefore, that loss of *Zic1/4* function does not grossly alter VZ patterning or proliferation, but we cannot exclude more subtle abnormalities.

DEVELOPMENT
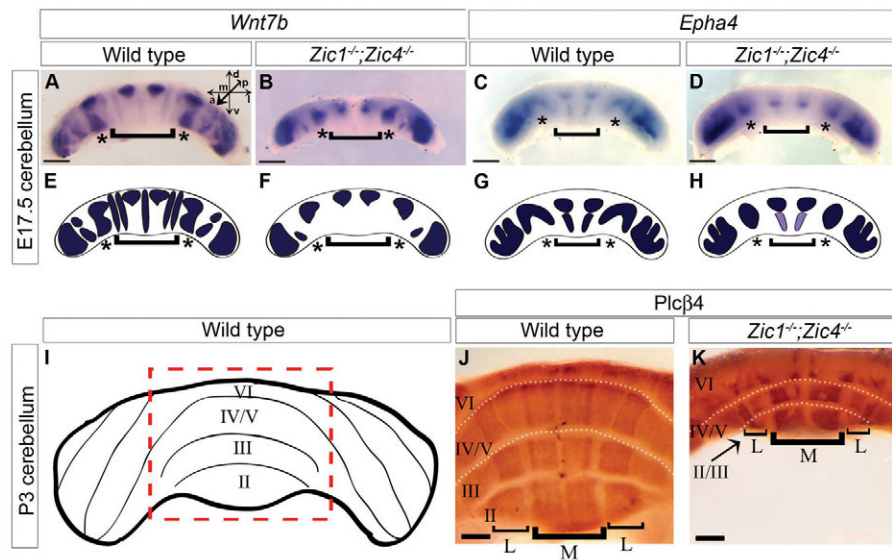
Fig. 6. Embryonic and neonatal mispatterning of Zic mutant cerebella correlates with adult foliation defects. (**A-D**) Anterior views of in situ hybridization for *Wnt7b* (A,B) and *Epha4* (C,D) in whole E17.5 cerebella. Wild-type parasagittal stripe patterns (A,C). Anterior stripes were reduced in size or absent in *Zic1⁻/⁻;Zic4⁻/⁻* cerebella (B,D). d, dorsal; v, ventral; a, anterior; p, posterior; m, medial; l, lateral. (**E-H**) Diagrams depict normal (E,G) and disrupted expression patterns (F,H). Regions of stripe differences are indicated by asterisks and brackets in A-H. (**I**) The anterior surface of a P3 cerebellum with vermis highlighted (red dotted box). (**J,K**) Anterior vermis views of anti-Plcβ4 whole-mount antibody staining of P3 cerebella. Wild-type cerebellar vermis (J) with four major parasagittal stripes of expression (brackets; M, medial; L, lateral) perpendicular to folia (roman numerals). Fissures (dotted lines in J and K) excluded antibody penetration and produced areas with no visible staining between lobes. *Zic1⁻/⁻;Zic4⁻/⁻* (K) cerebella lacked one anterior lobule and remaining stripes were abnormally patterned. The medial stripes of lobe II/III were relatively unaffected, but the lateral stripes were much narrower compared with wild type. Lobe IV/V patterns were completely disrupted with irregularly shaped and bilaterally asymmetric regions of expression. Scale bars: 500 μm in A-D; 250 μm in J,K.

DISCUSSION

DWM is the most common congenital malformation of the human cerebellum, yet its genetic and developmental basis remain largely unknown (Aldinger et al., 2009; Grinberg et al., 2004; Jalali et al., 2008; McCormack et al., 2002; Parisi and Dobyns, 2003). The first characterized DWM locus encompasses the linked *ZIC1* and *ZIC4* genes on chromosome 3q24 and heterozygous co-deletion of *Zic1* and *Zic4* mouse genes causes a DWM-like phenotype, implicating these genes as the first DWM causative genes (Grinberg et al., 2004). Complete loss of *Zic1* in mice is known to cause cerebellar hypoplasia and foliation defects, specifically loss of an entire anterior lobe, as well as ataxia, growth retardation and decreased viability (Aruga et al., 1998). However, both our human DWM and mouse mutant data demonstrate that *Zic4* is also essential for normal cerebellar development and can function in combination with *Zic1*.

To delineate the developmental pathogenesis of *ZIC1/ZIX4*-dependent DWM, we examined mature and developing *Zic4⁻/⁻* and *Zic1⁻/⁻;Zic4⁻/⁻* cerebellar phenotypes and compared them with *Zic1⁻/⁻* mutants. We determined that *Zic1* and *Zic4* both have roles in the regulation of cerebellar size and cerebellar anlage patterning. During early postnatal development, *Zic1* and *Zic4* regulate GCP proliferation in the cerebellar EGL in a Shh-dependent manner. *Zic1* and *Zic4* have an additional function in regulating embryonic cerebellar anlage PC patterning and cerebellar foliation; this function, however, is Shh independent. Taken together our data, suggest that the DWM-like pathogenesis in *Zic1/4* mutant mice is the result of disruptions of multiple cerebellar developmental programs.

Zic1 and *Zic4* regulate proliferation to control Shh-mediated cerebellar growth

A postnatal growth deficit is a prominent feature of both *Zic1⁻/⁻* and *Zic1⁻/⁻;Zic4⁻/⁻* phenotypes. Cerebellar growth occurs mainly after birth in mice and is due to rapid EGL proliferation. Mitotic index measurements revealed that in *Zic1⁻/⁻* and *Zic1⁻/⁻;Zic4⁻/⁻* cerebella, proliferation was normal at P0 but significantly reduced at P1, explaining the reduced cerebellar size seen both at P5 and P20. EGL expansion is largely driven by Shh signaling from the underlying PC layer (Corrales et al., 2006; Lewis et al., 2004). We determined that PC expression of *Shh* and two other markers of PCs, *Calb1* and *Rora*, was normal. However, we observed decreased expression of the EGL-specific Shh target genes *Ptch1*, *Gli1* and *Mycn* in *Zic1⁻/⁻* and *Zic1⁻/⁻;Zic4⁻/⁻* cerebella, indicating abnormalities in reception and/or processing of the Shh signal in EGL cells, rather than defects in PC Shh signaling. Decreased Shh target expression was observed at E17.5, preceding obvious size differences, and reduced expression was observed again at P1, which correlated with reduced EGL proliferation at this stage. Interestingly, Shh downstream target gene expression in *Zic4⁻/⁻* mutants was normal at E17.5, but *Gli1* and *Ptch1* expression levels were reduced at P1. As *Zic4⁻/⁻* adult cerebella were not significantly smaller than wild type and EGL proliferation was not reduced at P1 in these mutants, our findings indicate either that *Zic4* is not required for regulation of all Shh target genes, or that the loss of *Zic4* is partially compensated by additional factors such as other Zic family members. A more detailed analysis of additional Shh target genes will be necessary to determine the extent to which each Zic gene participates in Shh-mediated developmental processes.
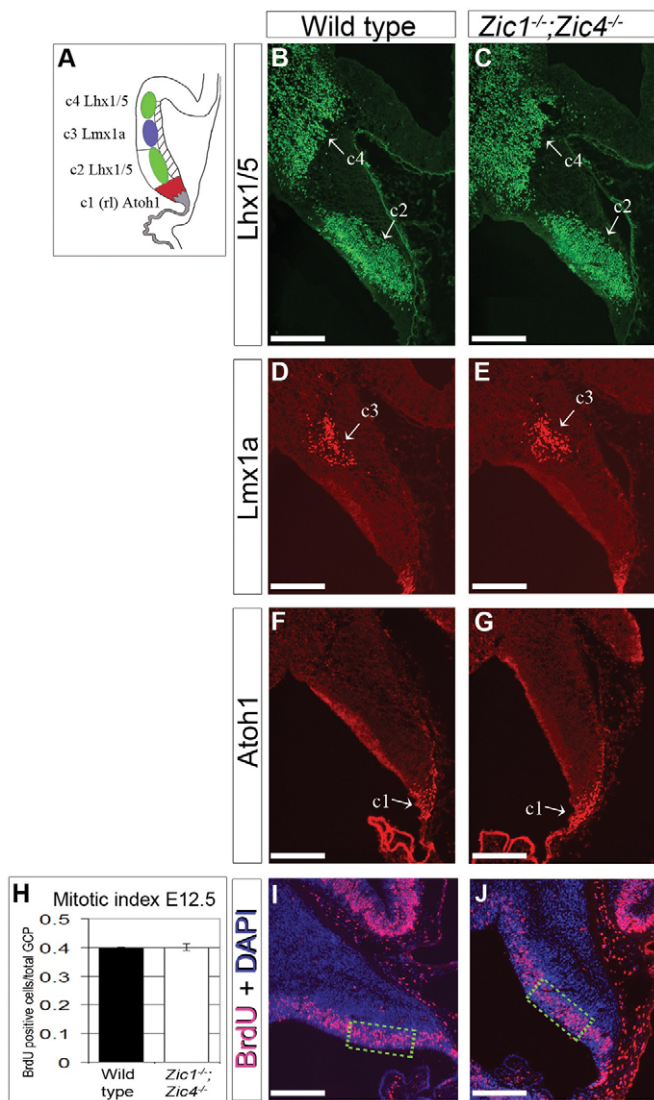
Fig. 7. Pattering of the cerebellar anlage is normal at E12.5.
(**A**) Diagram of a sagittal section through dorsal rhombomere 1 at E12.5 showing relative positions of cell populations c1-4. (**B-G**) Antibody staining of sagittal sections showed populations of Lhx1/5-positive c2/c4 cells (B,C), Lmx1a positive c3 cells (D,E) and Atoh1 positive c1 (rl=rhombic lip) cells (F,G) to be the same in wild-type and $Zic1^{-/-};Zic4^{-/-}$ E12.5 cerebella. (**H-J**) BrdU incorporation analysis showed that proliferation was not grossly changed in the ventricular zone of $Zic1^{-/-};Zic4^{-/-}$ cerebella at E12.5. Scale bars: 500 µm in B-G,I,J. Data are mean±s.e.m. Outlined areas in I, J indicate regions of cell counts.

It has been hypothesized that Zic proteins are downstream effectors in the Shh pathway based on the similarity between Zic and Gli ZF domains (Mizugishi et al., 2001). Our observation of downregulated Shh target genes *Ptch1*, *Gli1* and *Mycn* supports this hypothesis. To directly test a possible genetic interaction in vivo, we generated $Zic1^{+/-};Zic4^{+/-};Shh^{+/-}$ triple heterozygotes. We determined that loss of one allele of *Shh* in the $Zic1^{+/-};Zic4^{+/-}$ background was sufficient to cause additional reduction of cerebellar size, comparable with that observed in $Zic1^{-/-};Zic4^{-/-}$ cerebella. This size reduction was significant compared with changes observed in $Shh^{+/-}$ and $Zic1^{+/-};Zic4^{+/-}$ animals. QRT-PCR also confirmed that Shh target genes were downregulated in triple

heterozygous cerebella at E17.5 to a degree comparable with that of $Zic1^{-/-};Zic4^{-/-}$ mutants and further indicated that a 20-30% reduction of Shh target gene expression is sufficient to significantly reduce EGL proliferation and cerebellar size.

Together, our data provide the first direct in vivo confirmation of an interaction between *Zic1*, *Zic4* and the Shh pathway; however, the mechanism remains unclear. Zic1 can preferentially bind to Gli DNA-binding sequences through its ZF domains, and both Zic1 and Zic4 can drive reporter expression from plasmids containing Gli-binding sites (Koyabu et al., 2001; Mizugishi et al., 2001). In addition, Zic and Gli proteins can directly interact via their ZF domains in co-immunoprecipitation assays (Koyabu et al., 2001). Therefore, Zic proteins may also modulate Gli function in a DNA-independent manner. ChIP assays that compare EGL cells from wild type, $Zic1^{-/-}$, $Zic4^{-/-}$ and $Zic1^{-/-};Zic4^{-/-}$ mutant cerebella will be necessary to determine whether *Ptch1*, *Gli1* and *Mycn* are indeed direct Zic targets. It is also plausible that Zic proteins regulate the Shh pathway indirectly. For example, Wnts have been shown to modulate the Shh pathway by regulating *Gli2* and *Gli3* in avian somites (Borycki et al., 2000) and our expression data at E17.5 indicate that *Wnt1* downregulation may contribute to the *Zic1/4* cerebellar phenotype. Although we can conclude that Fgfs and Bmps are not significantly affected in our mutants, genome-wide expression microarray analyses will determine whether other pathways, such as the Notch signaling pathway (Aruga et al., 2002b), are also effectors of Zic1 and Zic4 function in the developing EGL.

The roles of *Zic1* and *Zic4* in cerebellar foliation and PC patterning

In addition to regulating size, *Zic1* and *Zic4* are required for normal foliation of the anterior cerebellar vermis. In $Zic1^{-/-}$ and $Zic1^{-/-};Zic4^{-/-}$ mutants, we observed abnormal positioning of the preculminate fissure, resulting in reduction of the anterobasal domain in mutant cerebella. The relationship between cerebellar growth and foliation is complex as the two processes occur during roughly the same developmental period and are often both affected in cerebellar mutants (Alcaraz et al., 2006; Cheng et al., 2010; Corrales et al., 2006; Lewis et al., 2004; Satokata et al., 2000; Sillitoe and Joyner, 2007). Furthermore, analysis of conditional mutants in the Shh pathway has shown that reduction of Shh signaling produces a range of foliation phenotypes in addition to size deficits (Corrales et al., 2006). Careful analysis of two Shh-depleted mouse lines demonstrated that Zic mutant foliation defects arose earlier and were more severe than those produced by loss of *Shh*. $Zic1^{+/-};Zic4^{+/-};Shh^{+/-}$ cerebella, which had reduced *Shh* expression, were small but had the correct number of anterior folia. *Gli2*-cko mice, from which cerebellar Shh signaling is functionally removed, were severely hypoplastic with almost no GCs, but also had the correct number of anterior folia. *Gli2*-cko cerebella also had correct positioning of the preculminate fissure, providing even more compelling evidence that the anterior foliation defects seen in $Zic1^{-/-}$ and $Zic1^{-/-};Zic4^{-/-}$ mutants are independent of the Shh pathway.

Very little is known of mechanisms that regulate cardinal fissure positioning in the developing cerebellum and our data add *Zic1* and *Zic4* to the short list of genes known to regulate cardinal fissure placement (Cheng et al., 2010). Expression of *Zic1* and *Zic4* is relatively uniform across the cerebellar anlage from E17.5 to P0 when these fissures form; thus, Zic1 and Zic4 must interact with other factors to read positional coordinates in the anterior cerebellum. Differentiating PCs are one potential source of this

information. Parasagittal clusters of PCs can be identified during perinatal development by expression of genes such as *En2*, *En1*, *Wnt7b*, *Plcb4* and several members of the Eph family of receptors (Blanco et al., 2002; Karam et al., 2002; Larouche and Hawkes, 2006; Millen et al., 1995; Sarna et al., 2006). This PC heterogeneity is thought to encode a topographic map for incoming cerebellar afferents (Sillitoe and Joyner, 2007). Cerebellar foliation defects are linked to abnormal afferent patterning in the posterior lobes. This has led to speculation that foliation and afferent innervation are developmentally related (Millen et al., 1995), although there is also evidence that folial and PC patterning can be dissociated (Sillitoe et al., 2008).

We determined that a subset of genes that delineate parasagittal PC compartments (*Epha4*, *Wnt7b*) had altered expression in *Zic1*$^{-/-}$ and *Zic1*$^{-/-}$;*Zic4*$^{-/-}$ mutant cerebella at E17.5, specifically in anterior regions where later abnormal foliation was evident. Furthermore, aberrant PC topography in this region was not transient, but remained disrupted at P3, as evidenced by altered *Plcb4* expression patterns in *Zic1*$^{-/-}$ and *Zic1*$^{-/-}$;*Zic4*$^{-/-}$ mutant cerebella. Thus, our data reveal a role for *Zic1* and *Zic4* in PC patterning of the anterior vermis. Notably, *Epha4* and *Wnt7b* stripe patterns were normal in *Zic1*$^{+/-}$;*Zic4*$^{+/-}$;*Shh*$^{+/-}$, Gli2-cko and Smo-cko mutants at E17.5, indicating that this Zic function is also independent of the Shh pathway. Although there is no direct evidence of a causal relationship between PC parasagittal stripes and cerebellar foliation, our findings that both foliation and PC patterning are disrupted in the anterior vermis in our Zic mutants are suggestive and clearly merit further study.

The developmental basis of the cerebellar anlage patterning phenotypes we observed remains unclear. One possibility is that loss of Zic1 function in the cerebellar VZ disrupts the generation of a subset of PCs destined for the anterior vermis. This hypothesis is based on the observation that following adenoviral labeling of PC progenitors between E10.5 and E12.5, clonally related PCs are positioned in parasagittal stripes in the adult cerebellum. Organization of clonally related PCs is established by late embryonic development and parasagittal stripe domains correlate with expression of stripe markers such as *Epha4* and *Wnt7b*, indicating that PC fate choices are specified at their genesis. It is notable that adenoviral ablation of PCs born on E12.5 disrupts cerebellar parasagittal stripe organization embryonically and produces abnormal foliation in the adult cerebellum (Hashimoto and Mikoshiba, 2003). As *Zic4* is not expressed in the cerebellar VZ, this may explain why *Zic4*$^{-/-}$ mutants do not have abnormal parasagittal stripe or folial patterning. Recent work has shown that Shh in fourth ventricle cerebrospinal fluid is required for normal proliferation within the cerebellar VZ from E12.5 onwards (Huang et al., 2010). However, we did not detect proliferation abnormalities in the *Zic1*$^{-/-}$;*Zic4*$^{-/-}$ cerebellar VZ at E12.5 when substantial numbers of PCs are generated, indicating that *Zic1* is dispensable for Shh-mediated VZ proliferation at this stage.

PC topography abnormalities may also reflect a requirement for *Zic1* in early differentiating neurons to control their migratory pathways into the anterior vermis. This is supported by the recent observation that *Zic1* is required for correct migration to and positioning of differentiating pontine gray neurons in the brainstem (Dipietrantonio and Dymecki, 2009). A detailed analysis of the fates of PC birth cohorts and their migration patterns within the cerebellar anlage will be required to determine whether a subset of PCs is absent, mis-specified or migrates incorrectly within developing Zic mutant cerebella.

Extracerebellar roles for *Zic1* and *Zic4*?

Through genetic and developmental analyses, we have determined that *Zic1* and *Zic4* have multiple roles within the developing cerebellum. Notably, loss of *Zic1* and *Zic4* produces a DWM-like phenotype through a mechanism distinct from that which we have reported to be caused by deletion of *Foxc1*, the only other known DWM causative gene identified to date. *Foxc1*, which is expressed in the head mesenchyme surrounding the cerebellar anlage, regulates expression of secreted growth factors required for rhombic lip development, but has no apparent direct function within the developing cerebellum (Aldinger et al., 2009). By contrast, here, we have detailed multiple roles for *Zic1* and *Zic4* within the cerebellar anlage. It is interesting to note, however, that both Zic1 and Zic4 are also expressed in the posterior fossa mesenchyme [Fig. 2I,J and Aruga et al. (Aruga et al., 1994)]. Recent work has shown that *Foxc1* is significantly downregulated in *Zic1*$^{-/-}$;*Zic3*$^{Bn/Y}$ mutant forebrain meninges (Inoue et al., 2008). The role of mesenchymal signaling in cerebellar development is not well understood, but these data suggest that, in addition to the proliferation and patterning roles played by *Zic1* and *Zic4* in the cerebellar anlage, these genes may have additional roles in the posterior fossa mesenchyme that are important for cerebellar development. This link between all known DWM genes bears further inquiry.

Competing interests statement
The authors declare no competing financial interests.

Supplementary material
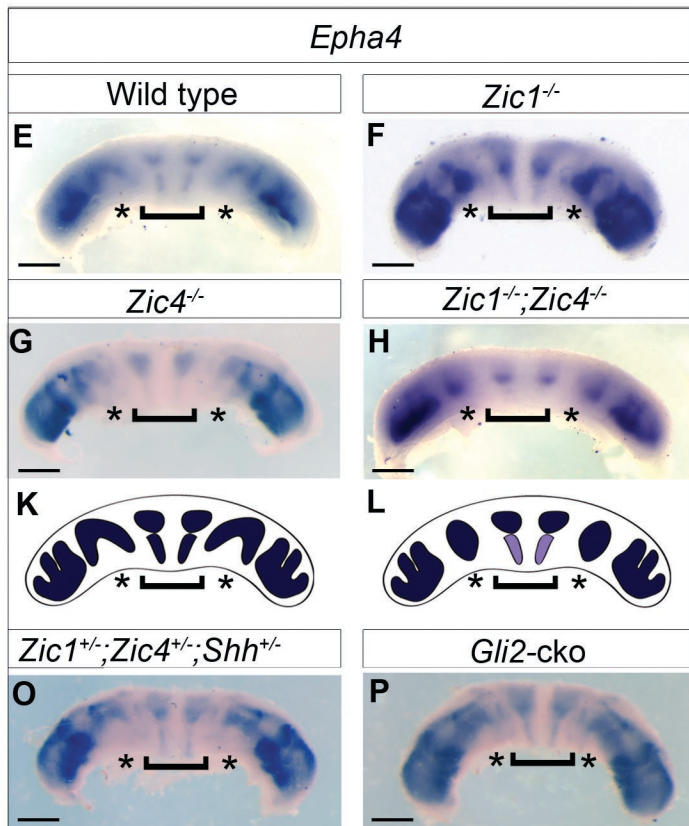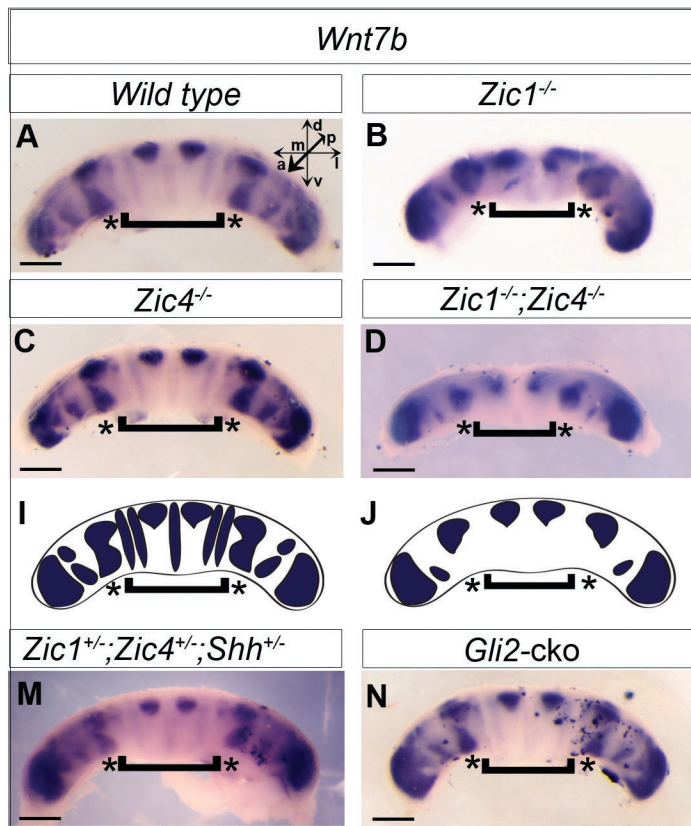Supplementary material for this article is available at
http://dev.biologists.org/lookup/suppl/doi:10.1242/dev.054114/-/DC1

References
Alcaraz, W. A., Gold, D. A., Raponi, E., Gent, P. M., Concepcion, D. and Hamilton, B. A. (2006). Zfp423 controls proliferation and differentiation of neural precursors in cerebellar vermis formation. *Proc. Natl. Acad. Sci. USA* **103**, 19424-19429.

Aldinger, K. A., Lehmann, O. J., Hudgins, L., Chizhikov, V. V., Bassuk, A. G., Ades, L. C., Krantz, I. D., Dobyns, W. B. and Millen, K. J. (2009). FOXC1 is required for normal cerebellar development and is a major contributor to chromosome 6p25.3 Dandy-Walker malformation. *Nat. Genet.* **41**, 1037-1042.

Aruga, J., Yokota, N., Hashimoto, M., Furuichi, T., Fukuda, M. and Mikoshiba, K. (1994). A novel zinc finger protein, zic, is involved in neurogenesis, especially in the cell lineage of cerebellar granule cells. *J. Neurochem.* **63**, 1880-1890.

Aruga, J., Minowa, O., Yaginuma, H., Kuno, J., Nagai, T., Noda, T. and Mikoshiba, K. (1998). Mouse Zic1 is involved in cerebellar development. *J. Neurosci.* **18**, 284-293.

Aruga, J., Inoue, T., Hoshino, J. and Mikoshiba, K. (2002a). Zic2 controls cerebellar development in cooperation with Zic1. *J. Neurosci.* **22**, 218-225.

Aruga, J., Tohmonda, T., Homma, S. and Mikoshiba, K. (2002b). Zic1 promotes the expansion of dorsal neural progenitors in spinal cord by inhibiting neuronal differentiation. *Dev. Biol.* **244**, 329-341.

Aruga, J., Ogura, H., Shutoh, F., Ogawa, M., Franke, B., Nagao, S. and Mikoshiba, K. (2004). Locomotor and oculomotor impairment associated with cerebellar dysgenesis in Zic3-deficient (Bent tail) mutant mice. *Eur. J. Neurosci.* **20**, 2159-2167.

Barkovich, A. J., Millen, K. J. and Dobyns, W. B. (2009). A developmental and genetic classification of mid-hindbrain malformations. *Brain* **132**, 3199-3230.

Behesti, H. and Marino, S. (2009). Cerebellar granule cells: insights into proliferation, differentiation, and role in medulloblastoma pathogenesis. *Int. J. Biochem. Cell Biol.* **41**, 435-445.

Blanco, M. J., Pena-Melian, A. and Nieto, M. A. (2002). Expression of EphA receptors and ligands during chick cerebellar development. *Mech. Dev.* **114**, 225-229.

Borycki, A., Brown, A. M. and Emerson, C. P. (2000). Shh and Wnt signaling pathways converge to control Gli gene activation in avian somites. *Development* **127**, 20755-20787.

Cheng, Y., Sudarov, A., Szulc, K. U., Sgaier, S. K., Stephen, D., Turnbull, D. H. and Joyner, A. L. (2010). The Engrailed homeobox genes determine the different foliation patterns in the vermis and hemispheres of the mammalian cerebellum. *Development* **137**, 519-529.

Chiang, C., Litingtung, Y., Lee, E., Young, K. E., Corden, J. L., Westphal, H. and Beachy, P. A. (1996). Cyclopia and defective axial patterning in mice lacking Sonic hedgehog gene function. *Nature* **383**, 407-413.

Chizhikov, V. V. and Millen, K. J. (2004). Control of roof plate development and signaling by Lmx1b in the caudal vertebrate CNS. *J. Neurosci.* **24**, 5694-5703.

Chizhikov, V. V., Lindgren, A. G., Currle, D. S., Rose, M. F., Monuki, E. S. and Millen, K. J. (2006). The roof plate regulates cerebellar cell-type specification and proliferation. *Development* **133**, 2793-2804.

Corrales, J. D., Blaess, S., Mahoney, E. M. and Joyner, A. L. (2006). The level of sonic hedgehog signaling regulates the complexity of cerebellar foliation. *Development* **133**, 1811-1821.

Dipietrantonio, H. J. and Dymecki, S. M. (2009). Zic1 levels regulate mossy fiber neuron position and axon laterality choice in the ventral brain stem. *Neuroscience* **162**, 560-573.

Goldowitz, D. and Hamre, K. (1998). The cells and molecules that make a cerebellum. *Trends Neurosci.* **21**, 375-382.

Grinberg, I., Northrup, H., Ardinger, H., Prasad, C., Dobyns, W. B. and Millen, K. J. (2004). Heterozygous deletion of the linked genes ZIC1 and ZIC4 is involved in Dandy-Walker malformation. *Nat. Genet.* **36**, 1053-1055.

Hashimoto, M. and Mikoshiba, K. (2003). Mediolateral compartmentalization of the cerebellum is determined on the "birth date" of Purkinje cells. *J. Neurosci.* **23**, 11342-11351.

Huang, X., Liu, J., Ketova, T., Fleming, J. T., Grover, V. K., Cooper, M. K., Litingtung, Y. and Chiang, C. (2010). Transventricular delivery of Sonic hedgehog is essential to cerebellar ventricular zone development. *Proc. Natl. Acad. Sci. USA* **107**, 8422-8427.

Inoue, T., Ogawa, M., Mikoshiba, K. and Aruga, J. (2008). Zic deficiency in the cortical marginal zone and meninges results in cortical lamination defects resembling those in type II lissencephaly. *J. Neurosci.* **28**, 4712-4725.

Ishiguro, A., Inoue, T., Mikoshiba, K. and Aruga, J. (2004). Molecular properties of Zic4 and Zic5 proteins: functional diversity within Zic family. *Biochem. Biophys. Res. Commun.* **324**, 302-307.

Jalali, A., Aldinger, K. A., Chary, A., McLone, D. G., Bowman, R. M., Le, L. C., Jardine, P., Newbury-Ecob, R., Mallick, A., Jafari, N. et al. (2008). Linkage to chromosome 2q36.1 in autosomal dominant Dandy-Walker malformation with occipital cephalocele and evidence for genetic heterogeneity. *Hum. Genet.* **123**, 237-245.

Karam, S. D., Dottori, M., Ogawa, K., Henderson, J. T., Boyd, A. W., Pasquale, E. B. and Bothwell, M. (2002). EphA4 is not required for Purkinje cell compartmentation. *Brain Res. Dev. Brain Res.* **135**, 29-38.

Kimmel, R. A., Turnbull, D. H., Blanquet, V., Wurst, W., Loomis, C. A. and Joyner, A. L. (2000). Two lineage boundaries coordinate vertebrate apical ectodermal ridge formation. *Genes Dev.* **14**, 1377-1389.

Koyabu, Y., Nakata, K., Mizugishi, K., Aruga, J. and Mikoshiba, K. (2001). Physical and functional interactions between Zic and Gli proteins. *J. Biol. Chem.* **276**, 6889-6892.

Larouche, M. and Hawkes, R. (2006). From clusters to stripes: the developmental origins of adult cerebellar compartmentation. *Cerebellum* **5**, 77-88.

Lewis, P. M., Gritli-Linde, A., Smeyne, R., Kottmann, A. and McMahon, A. P. (2004). Sonic hedgehog signaling is required for expansion of granule neuron precursors and patterning of the mouse cerebellum. *Dev. Biol.* **270**, 393-410.

Li, J. Y., Lao, Z. and Joyner, A. L. (2002). Changing requirements for Gbx2 in development of the cerebellum and maintenance of the mid/hindbrain organizer. *Neuron* **36**, 31-43.

Liebl, D. J., Morris, C. J., Henkemeyer, M. and Parada, L. F. (2003). mRNA expression of ephrins and Eph receptor tyrosine kinases in the neonatal and adult mouse central nervous system. *J. Neurosci. Res.* **71**, 7-22.

McCormack, W. M., Jr, Shen, J. J., Curry, S. M., Berend, S. A., Kashork, C., Pinar, H., Potocki, L. and Bejjani, B. A. (2002). Partial deletions of the long arm of chromosome 13 associated with holoprosencephaly and the Dandy-Walker malformation. *Am. J. Med. Genet.* **112**, 384-389.

Merzdorf, C. S. (2007). Emerging roles for zic genes in early development. *Dev. Dyn.* **236**, 922-940.

Millen, K. J., Hui, C. C. and Joyner, A. L. (1995). A role for En-2 and other murine homologues of Drosophila segment polarity genes in regulating positional information in the developing cerebellum. *Development* **121**, 3935-3945.

Mizugishi, K., Aruga, J., Nakata, K. and Mikoshiba, K. (2001). Molecular properties of Zic proteins as transcriptional regulators and their relationship to GLI proteins. *J. Biol. Chem.* **276**, 2180-2188.

Nagai, T., Aruga, J., Takada, S., Gunther, T., Sporle, R., Schughart, K. and Mikoshiba, K. (1997). The expression of the mouse Zic1, Zic2, and Zic3 gene suggests an essential role for Zic genes in body pattern formation. *Dev. Biol.* **182**, 299-313.

Parisi, M. A. and Dobyns, W. B. (2003). Human malformations of the midbrain and hindbrain: review and proposed classification scheme. *Mol. Genet. Metab.* **80**, 36-53.

Parr, B. A., Shea, M. J., Vassileva, G. and McMahon, A. P. (1993). Mouse Wnt genes exhibit discrete domains of expression in the early embryonic CNS and limb buds. *Development* **119**, 247-261.

Pogoriler, J., Millen, K. J., Utset, M. and Du, W. (2006). Loss of cyclin D1 impairs cerebellar development and suppresses medulloblastoma formation. *Development* **133**, 3929-3937.

Ruiz i Altaba, A., Palma, V. and Dahmane, N. (2002). Hedgehog-Gli signalling and the growth of the brain. *Nat. Rev. Neurosci.* **3**, 24-33.

Sarna, J. R., Marzban, H., Watanabe, M. and Hawkes, R. (2006). Complementary stripes of phospholipase Cbeta3 and Cbeta4 expression by Purkinje cell subsets in the mouse cerebellum. *J. Comp. Neurol.* **496**, 303-313.

Satokata, I., Ma, L., Ohshima, H., Bei, M., Woo, I., Nishizawa, K., Maeda, T., Takano, Y., Uchiyama, M., Heaney, S. et al. (2000). Msx2 deficiency in mice causes pleiotropic defects in bone growth and ectodermal organ formation. *Nat. Genet.* **24**, 391-395.

Sillitoe, R. V. and Hawkes, R. (2002). Whole-mount immunohistochemistry: a high-throughput screen for patterning defects in the mouse cerebellum. *J. Histochem. Cytochem.* **50**, 235-244.

Sillitoe, R. V. and Joyner, A. L. (2007). Morphology, molecular codes, and circuitry produce the three-dimensional complexity of the cerebellum. *Annu. Rev. Cell Dev. Biol.* **23**, 549-577.

Sillitoe, R. V., Stephen, D., Lao, Z. and Joyner, A. L. (2008). Engrailed homeobox genes determine the organization of Purkinje cell sagittal stripe gene expression in the adult cerebellum. *J. Neurosci.* **28**, 12150-12162.

Spring, S., Lerch, J. P. and Henkelman, R. M. (2007). Sexual dimorphism revealed in the structure of the mouse brain using three-dimensional magnetic resonance imaging. *Neuroimage* **35**, 1424-1433.

Vaillant, C. and Monard, D. (2009). SHH pathway and cerebellar development. *Cerebellum* **8**, 291-301.

Wild type | Zic4+/- | Zic1+/- | Zic1+/-;Zic4+/-

Zic4-/- | Zic1+/-;Zic4-/-

Zic1-/- | Zic1-/-;Zic4+/- | Zic1-/-;Zic4-/-

Wnt7b

Epha4

A — Wild type

B — *Zic1*^{-/-}

C — *Zic4*^{-/-}

D — *Zic1*^{-/-};*Zic4*^{-/-}

E — Wild type

F — *Zic1*^{-/-}

G — *Zic4*^{-/-}

H — *Zic1*^{-/-};*Zic4*^{-/-}

I

J

K

L

M — *Zic1*^{+/-};*Zic4*^{+/-};*Shh*^{+/-}

N — *Gli2*-cko

O — *Zic1*^{+/-};*Zic4*^{+/-};*Shh*^{+/-}

P — *Gli2*-cko

Wild type   *Zic4*⁻ᐟ⁻   *Zic1*⁻ᐟ⁻   *Zic1*⁻ᐟ⁻;*Zic4*⁻ᐟ⁻